

Revisiting radiative decays $h_c \rightarrow \gamma\eta^{(\prime)}$ with the Bethe-Salpeter equation under covariant instantaneous ansatz

Jun-Kang He^{*} and Chao-Jie Fan[†]

Institute of Particle Physics and Key Laboratory of Quark and Lepton Physics (MOE),
Central China Normal University, Wuhan, Hubei 430079, China

Abstract

The P -wave charmonium decays $h_c \rightarrow \gamma\eta^{(\prime)}$ are revisited in the Bethe-Salpeter equation framework, where the bound state properties of h_c are described by its Bethe-Salpeter wave function with covariant instantaneous ansatz. By using the helicity projector, we evaluate analytically the one-loop integrals with the internal momentum of h_c kept, and the branching ratios $\mathcal{B}(h_c \rightarrow \gamma\eta^{(\prime)})$ are found to be insensitive to the light quark masses and the shapes of $\eta^{(\prime)}$ distribution amplitudes. Our numerical results show that the contributions of the gluonic content of $\eta^{(\prime)}$ are as important as those of the quark-antiquark content of $\eta^{(\prime)}$. Comparing to the results with the zero-binding approximation, we find that the relativistic corrections related to the internal momentum of h_c are almost negligible in the P -wave charmonium decays $h_c \rightarrow \gamma\eta^{(\prime)}$. As a crossing check, by the ratios $R_{h_c} = \mathcal{B}(h_c \rightarrow \gamma\eta)/\mathcal{B}(h_c \rightarrow \gamma\eta')$ and $\Gamma(\eta \rightarrow \gamma\gamma)/\Gamma(\eta' \rightarrow \gamma\gamma)$, we obtain the mixing angle $\phi = 33.8^\circ \pm 2.4^\circ$, which is almost the same as the value extracted from the R_{h_c} with the zero-binding approximation.

^{*}hejk@mails.ccnu.edu.cn

[†]fancj@mails.ccnu.edu.cn

1 Introduction

The hadronic decays of charmonia have played important roles for our understanding of quantum chromodynamics (QCD), especially the interplay of perturbative quantum chromodynamics (pQCD) and nonperturbative QCD, since the first charmonium state J/ψ was observed [1, 2]. One of the interesting topics is the Okubo-Zweig-Iizuka (OZI)-suppressed radiative decays of charmonia to the light mesons $\eta^{(\prime)}$, since these decays are closely related to the issue of $\eta - \eta'$ mixing, which is an important ingredient for understanding many phenomena related to the mesons $\eta^{(\prime)}$. In recent years, there are more and more experimental measurements on these processes, such as $J/\psi \rightarrow \gamma\eta^{(\prime)}$ [3–6], $\psi' \rightarrow \gamma\eta^{(\prime)}$ [5, 7, 8], $\psi(3770) \rightarrow \gamma\eta^{(\prime)}$ [5] and $h_c \rightarrow \gamma\eta^{(\prime)}$ [9]. On the theoretical aspect, the S -wave charmonium decays $J/\psi \rightarrow \gamma\eta^{(\prime)}$ have been investigated in various approaches [10–18]. By the ratio $R_{J/\psi} = \mathcal{B}(J/\psi \rightarrow \gamma\eta')/\mathcal{B}(J/\psi \rightarrow \gamma\eta)$, the mixing angle was obtained $\phi = 39.3^\circ \pm 1.0^\circ$ [19] with nonperturbative matrix elements $\langle 0 | G_{\mu\nu}^a \tilde{G}^{a,\mu\nu} | \eta^{(\prime)} \rangle$ and $\phi = 33.9^\circ \pm 0.6^\circ$ [18] with pQCD. For the P -wave charmonium decays $h_c \rightarrow \gamma\eta^{(\prime)}$, the situation seems more complex, since the higher Fock-state contributions and the relativistic corrections may become important. As is well known, infra-red divergences are encountered in the inclusive P -wave charmonium decays with the zero-binding approximation [20–23], and these divergences, which can be replaced by a logarithm of the confinement radius [20–22] or the radius of the bound state [23], indicate that the nonperturbative effects beyond those contained in the derivative of the nonrelativistic wave function at the origin $|R'(0)|$ may play a key role. It is worth noting that these divergences can also be removed in the framework of nonrelativistic QCD [24, 25] with considering the higher Fock-state contributions. In the literature, the P -wave charmonium decays $h_c \rightarrow \gamma\eta^{(\prime)}$ have been studied in Refs. [26, 27]. And it was found that the calculations of the branching ratios $\mathcal{B}(h_c \rightarrow \gamma\eta^{(\prime)})$ are infra-red safe and the predicted $\mathcal{B}(h_c \rightarrow \gamma\eta^{(\prime)})$ are comparable to the experimental measurements [9]. However, in both of these two works, the relativistic corrections related to the internal momentum of the P -wave charmonium h_c had been neglected in the calculation of the hard kernels, and all the nonperturbative effects are absorbed in $|R'_{h_c}(0)|$ with the Taylor expansion of the hard kernels up to the linear terms in the nonrelativistic limit. As pointed out in Refs. [28–37], even though there are no infra-red divergences with the leading order approximation in the exclusive P -wave charmonium decays, the relativistic effects as well as the higher Fock-state are also significant

to these decays.

In order to make clear the relativistic corrections for the P -wave charmonium decays $h_c \rightarrow \gamma\eta^{(\prime)}$, one can employ the Bethe-Salpeter (B-S) equation framework, where the internal momentum of h_c is retained both in the soft bound state wave function and the hard kernel. With the B-S equation under covariant instantaneous ansatz (CIA) [38–40], we revisit the radiative decays $h_c \rightarrow \gamma\eta^{(\prime)}$ in this work. For the P -wave charmonium h_c , the B-S wave function, which describes the bound state properties of h_c , is adopted. For the final light mesons $\eta^{(\prime)}$, light-cone distribution amplitudes (DAs) are used because of the large momentum transfer. The $\eta - \eta'$ mixing is taken as the FKS scheme [19] and the contribution of the quark-antiquark content and that of the gluonic content are both taken into account. With the technique of helicity projector, we evaluate analytically the involved one-loop integrals with the internal momentum of h_c kept. Performing the integral over the internal momentum \hat{q} and the momentum fraction u , the dimensionless function H_q is found to be still insensitive to the light quark masses and the shapes of the $\eta^{(\prime)}$ DAs, which is accord with the conclusion obtained in our previous work [27] with the zero-binding approximation. So the theoretical uncertainties due to choices of $\eta^{(\prime)}$ DAs are negligible, and the mixing angle of the $\eta - \eta'$ system could be reliably determined in the our calculations.

The paper is organized as follows. The formalism for the decays $h_c \rightarrow \gamma\eta^{(\prime)}$ is presented in section 2. In section 3, we present our numerical results, and the final section is our summary. The expressions of the numerators involved in section 2 are given in appendix A.

2 Formalism for radiative decays $h_c \rightarrow \gamma\eta^{(\prime)}$

2.1 B-S equation under CIA

In this subsection, we briefly review the formulation of the framework with the B-S equation under CIA. For the charmonium, the B-S equation has the form [41–44]

$$S_F^{-1}(f)\Psi(K, q)S_F^{-1}(-\bar{f}) = \int \frac{d^4q'}{(2\pi)^4} \left[-i\mathcal{K}(K, q, q')\Psi(K, q') \right], \quad (2.1)$$

where $\mathcal{K}(K, q, q')$ represents the interaction kernel between the internal quark and antiquark, and $S_F(p) = i/(\not{p} - m_c + i\epsilon)$ represents the quark propagator with the c -quark mass m_c . The momenta of the quark and antiquark can be written as

$$f = \frac{K}{2} + q, \quad \bar{f} = \frac{K}{2} - q, \quad (2.2)$$

where q and K represent the internal momentum and the total momentum of the bound state respectively. For convenience, one can divide the internal momentum q into two parts. One part is the transverse component \hat{q} with $\hat{q} \cdot K = 0$, and the other is the longitudinal component $q_{\parallel}^{\mu} = \frac{q \cdot K}{M} K^{\mu}$, which is parallel to the total momentum K :

$$q^{\mu} = q_{\parallel}^{\mu} + \hat{q}^{\mu}. \quad (2.3)$$

Here both $q_K = \frac{q \cdot K}{M}$ and $\hat{q}^2 = q^2 - q_K^2$ are Lorentz invariant variables and M is the mass of the charmonium.

Under the CIA [38–40], the interaction kernel $\mathcal{K}(K, q, q')$ is taken to be dependent only on the momentum \hat{q}

$$\mathcal{K}(K, q, q') = V(\hat{q}, \hat{q}'). \quad (2.4)$$

Then the B-S wave function can be expressed as

$$\Psi(K, q) = -S_F(f)\Gamma(\hat{q})S_F(-\bar{f}), \quad (2.5)$$

where the hadron-quark vertex function reads

$$\Gamma(\hat{q}) = i \int \frac{d^4 q'}{(2\pi)^4} \mathcal{K}(\hat{q}, \hat{q}') \Psi(K, q') = \int \widetilde{d^3 q'} V(\hat{q}, \hat{q}') \psi(\hat{q}') \quad (2.6)$$

with $\psi(\hat{q}) = \frac{i}{2\pi} \int d^4 q_K \Psi(K, q)$ and $\widetilde{d^3 q'} = \frac{d^3 q'}{(2\pi)^3} \frac{M}{K^0}$. Using the projection operators

$$\Lambda_i^{\pm}(\hat{q}) = \frac{1}{2\omega} \left[\frac{\not{K}}{M} \omega \pm (-1)^{(i+1)} (m_c + \not{\hat{q}}) \right], \quad (2.7)$$

the propagators can be decomposed as

$$\begin{aligned}\frac{1}{f - m_c + i\epsilon} &= \frac{\Lambda_1^+(\hat{q})}{q_K + \frac{M}{2} - \omega + i\epsilon} + \frac{\Lambda_1^-(\hat{q})}{q_K + \frac{M}{2} + \omega - i\epsilon}, \\ \frac{1}{\bar{f} + m_c - i\epsilon} &= \frac{\Lambda_2^+(\hat{q})}{-q_K + \frac{M}{2} - \omega + i\epsilon} + \frac{\Lambda_2^-(\hat{q})}{-q_K + \frac{M}{2} + \omega - i\epsilon}\end{aligned}\quad (2.8)$$

with $\omega = \sqrt{\hat{m}^2 - \hat{q}^2}$. Performing the q_K -integration of Eq. (2.5), one can obtain [42–45]

$$\begin{aligned}(M - 2\omega)\psi^{++}(\hat{q}) &= -\Lambda_1^+(\hat{q})\Gamma(\hat{q})\Lambda_2^+(\hat{q}), \\ (M + 2\omega)\psi^{--}(\hat{q}) &= \Lambda_1^-(\hat{q})\Gamma(\hat{q})\Lambda_2^-(\hat{q}), \\ \psi^{+-}(\hat{q}) &= 0, \\ \psi^{-+}(\hat{q}) &= 0\end{aligned}\quad (2.9)$$

with $\psi^{\pm\pm}(\hat{q}) = \Lambda_1^{\pm}(\hat{q})\frac{\not{P}}{M}\psi(\hat{q})\frac{\not{P}}{M}\Lambda_2^{\pm}(\hat{q})$ and the Salpeter wave function

$$\psi(\hat{q}) = \psi^{++}(\hat{q}) + \psi^{+-}(\hat{q}) + \psi^{-+}(\hat{q}) + \psi^{--}(\hat{q}). \quad (2.10)$$

For the axial vector meson h_c , the Salpeter wave function with the Dirac structure up to $\mathcal{O}(\hat{q})$ terms can be approximately written as [43, 44, 46–48]

$$\psi(\hat{q}) = \hat{q} \cdot \varepsilon(K) \left[1 + \frac{\not{K}}{M} + \frac{\hat{q}\not{K}}{m_c M} \right] \gamma^5 f(\hat{q}^2), \quad (2.11)$$

where M and $\varepsilon(K)$ are the mass and the polarization vector of h_c respectively, and $f(\hat{q}^2)$ is a scalar wave function of \hat{q}^2 .

2.2 The contributions of the quark-antiquark content of $\eta^{(\prime)}$

For the quark-antiquark content of $\eta^{(\prime)}$, one of the leading order Feynman diagrams for the processes $h_c \rightarrow \gamma\eta^{(\prime)}$ is depicted in Fig. 1. Other five diagrams arise from permutations of the photon and gluon legs. And it is convenient to divide the invariant amplitude of $h_c \rightarrow \gamma\eta^{(\prime)}$ into two parts [27]. One part describes the effective coupling between h_c , a real photon and two virtual gluons, and the other one describes the effective coupling between $\eta^{(\prime)}$ and two virtual

gluons.

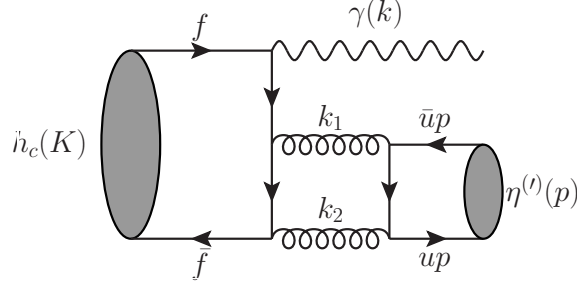


Figure 1: One typical Feynman diagram for $h_c \rightarrow \gamma \eta^{(l)}$ with the quark-antiquark content of $\eta^{(l)}$. Here the kinematical variables are labeled.

In the rest frame of h_c , the invariant amplitude of $h_c \rightarrow \gamma g^* g^*$ has the form [49]

$$\begin{aligned} \mathcal{A}^{\alpha\beta\mu\nu} \varepsilon_\alpha(K) \epsilon_\beta^*(k) \epsilon_\mu^*(k_1) \epsilon_\nu^*(k_2) &= -i\sqrt{3} \int \frac{d^4 q}{(2\pi)^4} \text{Tr} [\Psi(K, q) \mathcal{O}(\hat{q})] \\ &= -\sqrt{3} \int \frac{d^3 q}{(2\pi)^3} \text{Tr} [\psi(\hat{q}) \mathcal{O}(\hat{q})], \end{aligned} \quad (2.12)$$

where the factor $\sqrt{3}$ is included to account for the color properties of the quark-antiquark content and the hard kernel $\mathcal{O}(\hat{q})$ reads

$$\begin{aligned} \mathcal{O}(\hat{q}) &= iQ_c e g_s^2 \frac{\delta_{ab}}{6} \left[\not{\epsilon}^*(k_2) \frac{\frac{k_2 - k - k_1}{2} + \hat{q} + m_c}{\left(\frac{k_2 - k - k_1}{2} + \hat{q}\right)^2 - m_c^2} \not{\epsilon}^*(k) \frac{\frac{k_2 + k - k_1}{2} + \hat{q} + m_c}{\left(\frac{k_2 + k - k_1}{2} + \hat{q}\right)^2 - m_c^2} \not{\epsilon}^*(k_1) \right. \\ &\quad + \not{\epsilon}^*(k_1) \frac{\frac{k_1 - k - k_2}{2} + \hat{q} + m_c}{\left(\frac{k_1 - k - k_2}{2} + \hat{q}\right)^2 - m_c^2} \not{\epsilon}^*(k) \frac{\frac{k_1 + k - k_2}{2} + \hat{q} + m_c}{\left(\frac{k_1 + k - k_2}{2} + \hat{q}\right)^2 - m_c^2} \not{\epsilon}^*(k_2) \\ &\quad + \not{\epsilon}^*(k_2) \frac{\frac{k_2 - k_1 - k}{2} + \hat{q} + m_c}{\left(\frac{k_2 - k_1 - k}{2} + \hat{q}\right)^2 - m_c^2} \not{\epsilon}^*(k_1) \frac{\frac{k_2 + k_1 - k}{2} + \hat{q} + m_c}{\left(\frac{k_2 + k_1 - k}{2} + \hat{q}\right)^2 - m_c^2} \not{\epsilon}^*(k) \\ &\quad + \not{\epsilon}^*(k) \frac{\frac{k - k_2 - k_1}{2} + \hat{q} + m_c}{\left(\frac{k - k_2 - k_1}{2} + \hat{q}\right)^2 - m_c^2} \not{\epsilon}^*(k_2) \frac{\frac{k + k_2 - k_1}{2} + \hat{q} + m_c}{\left(\frac{k + k_2 - k_1}{2} + \hat{q}\right)^2 - m_c^2} \not{\epsilon}^*(k_1) \\ &\quad + \not{\epsilon}^*(k_1) \frac{\frac{k_1 - k_2 - k}{2} + \hat{q} + m_c}{\left(\frac{k_1 - k_2 - k}{2} + \hat{q}\right)^2 - m_c^2} \not{\epsilon}^*(k_2) \frac{\frac{k_1 + k_2 - k}{2} + \hat{q} + m_c}{\left(\frac{k_1 + k_2 - k}{2} + \hat{q}\right)^2 - m_c^2} \not{\epsilon}^*(k) \\ &\quad \left. + \not{\epsilon}^*(k) \frac{\frac{k - k_1 - k_2}{2} + \hat{q} + m_c}{\left(\frac{k - k_1 - k_2}{2} + \hat{q}\right)^2 - m_c^2} \not{\epsilon}^*(k_1) \frac{\frac{k + k_1 - k_2}{2} + \hat{q} + m_c}{\left(\frac{k + k_1 - k_2}{2} + \hat{q}\right)^2 - m_c^2} \not{\epsilon}^*(k_2) \right]. \end{aligned} \quad (2.13)$$

Here k , k_1 , k_2 and $\epsilon(k)$, $\epsilon(k_1)$, $\epsilon(k_2)$ stand for the momenta and polarization vectors of the photon and the gluons, respectively. It is worth noting that we have neglected the dependence

of q^0 in the hard kernels. As pointed out in Ref. [50], this treatment can be connected with the on-shell condition, which maintains the gauge invariance of the hard kernels but at the price of fixing \hat{q}^2 simultaneously. In order to study the relativistic effects related to the internal momentum of bound state, between the bound state description and the on-shell condition, the authors of Ref. [50] proposed a compromise[†], in which the internal momentum \hat{q} contained in the hard kernels is allowed to vary in accordance with the bound state wave function. Here we also make this compromise and take a P -wave harmonic oscillator wave function to describe the bound state properties of h_c :

$$f(\hat{q}^2) = N_A \left(\frac{2}{3}\right)^{\frac{1}{2}} \frac{1}{\pi^{\frac{3}{4}} \beta_A^{\frac{5}{2}}} |\mathbf{q}| e^{-\frac{\mathbf{q}^2}{2\beta_A^2}}, \quad (2.14)$$

where N_A is the normalization constant and the normalization equation of $f(\hat{q}^2)$ reads [44]

$$\int \frac{d^3q}{(2\pi)^3} \frac{4\omega \mathbf{q}^2}{3m_c M} f^2(\hat{q}^2) = 1. \quad (2.15)$$

The light-cone expansion of the matrix elements of the meson $\eta^{(\prime)}$ over quark and antiquark fields reads [54–56]

$$\langle \eta^{(\prime)}(p) | \bar{q}_\alpha(x) q_\beta(y) | 0 \rangle = \frac{i}{4} f_{\eta^{(\prime)}}^q (\not{p} \gamma_5)_{\beta\alpha} \int du e^{i(\bar{u}p \cdot y + up \cdot x)} \phi^q(u) + \dots, \quad (2.16)$$

where p represents the momentum of the $\eta^{(\prime)}$, the superscript $q = u, d, s$ denotes the flavor of the light quarks, the \dots stands for the high twist terms and the decay constants $f_{\eta^{(\prime)}}^q$ are defined as

$$\langle 0 | \bar{q}(0) \gamma_\mu \gamma_5 q(0) | \eta^{(\prime)}(p) \rangle = i f_{\eta^{(\prime)}}^q p_\mu. \quad (2.17)$$

Then one can obtain the coupling of $g^* g^* - \eta^{(\prime)}$ up to twist-3 level [57–59]:

$$\mathcal{M}^{\mu\nu} \epsilon_\mu(k_1) \epsilon_\nu(k_2) = -i(4\pi\alpha_s) \delta_{ab} \epsilon^{\mu\nu\rho\sigma} \epsilon_\mu(k_1) \epsilon_\nu(k_2) k_{1\rho} k_{2\sigma}$$

[†]In fact, when the internal momentum q is kept fully in the hard kernels in the B-S equation framework, the gauge invariance of the hard kernels also needs considering the higher Fock-state contributions [51–53], which is suppressed at least by the factor of $v_{cc}^2 \alpha_s$ in the decays $h_c \rightarrow \gamma \eta^{(\prime)}$ [26]. The compromise adopted in Ref. [50], in a sense, means the neglect of the higher Fock-state contributions.

$$\times \sum_{q=u,d,s} \frac{f_{\eta^{(\prime)}}^q}{6} \int_0^1 du \phi^q(u) \left(\frac{1}{\bar{u}k_1^2 + uk_2^2 - u\bar{u}p^2 - m_q^2} + (u \leftrightarrow \bar{u}) \right) \quad (2.18)$$

with $\bar{u} = 1 - u$. Here u is the momentum fraction carried by the quark, m_q is the mass of the quark ($q = u, d, s$) and m is the mass of $\eta^{(\prime)}$. The light-cone DA has the form [60]

$$\phi^q(u) = \phi_{AS}(u) \left[1 + \sum_{n=2,4,\dots} c_n^q(\mu) C_n^{\frac{3}{2}}(2u - 1) \right] \quad (2.19)$$

with the asymptotic form of DA $\phi_{AS}(u) = 6u(1 - u)$ and the Gegenbauer moments $c_n^q(\mu)$. In Table 1, we list three models of the DAs given in Ref. [60]. Schematically, we also show their shapes at the scale of $\mu_0 = m_c$ in Fig. 2.

Table 1: Gegenbauer coefficients of three sample models at the scale of $\mu_0 = 1 \text{ GeV}$.

Model	$c_2^q(\mu_0)$	$c_4^q(\mu_0)$	$c_2^g(\mu_0)$
I	0.10	0.10	-0.26
II	0.20	0.00	-0.31
III	0.25	-0.10	-0.25

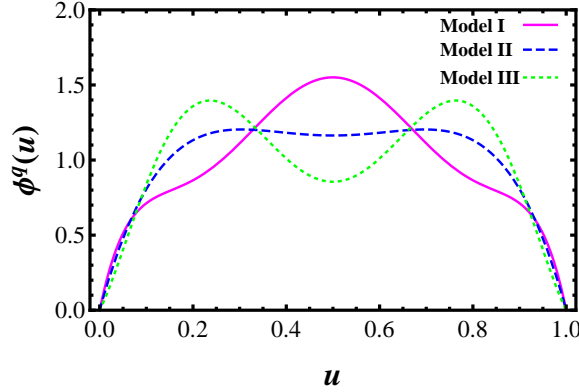


Figure 2: The shapes of the corresponding DAs at the scale of $\mu = m_c$.

The invariant amplitude of $h_c \rightarrow \gamma \eta^{(\prime)}$ can be obtained directly by contracting the two couplings $\mathcal{A}^{\alpha\beta\mu\nu}$ and $\mathcal{M}_{\mu\nu}$, inserting the gluon propagators and integrating over the loop momentum:

$$M_T = T^{\alpha\beta} \varepsilon_\alpha(K) \epsilon_\beta^*(k) = \frac{1}{2} \int \frac{d^4 k_1}{(2\pi)^4} \mathcal{A}^{\alpha\beta\mu\nu} \mathcal{M}_{\mu\nu} \frac{i}{k_1^2 + i\epsilon} \frac{i}{k_2^2 + i\epsilon} \varepsilon_\alpha(K) \epsilon_\beta^*(k). \quad (2.20)$$

By using Lorentz invariance, parity conservation and gauge invariance, one can obtain [11]

$$T^{\alpha\beta} \propto -g^{\alpha\beta} + \frac{k^\alpha K^\beta}{K \cdot k}, \quad (2.21)$$

i.e., there is only one independent helicity amplitude H_{QCD}^q :

$$T^{\alpha\beta} \varepsilon_\alpha(K) \epsilon_\beta^*(k) = H_{QCD}^q h^{\alpha\beta} \varepsilon_\alpha(K) \epsilon_\beta^*(k) \quad (2.22)$$

with

$$h^{\alpha\beta} = -g^{\alpha\beta} + \frac{k^\alpha K^\beta}{k \cdot K}. \quad (2.23)$$

With the help of the helicity projector [11]

$$\mathbb{P}^{\alpha\beta} = \frac{1}{2} h_{\alpha'\beta'}^* \left(-g^{\alpha\alpha'} + \frac{K^\alpha K^{\alpha'}}{M^2} \right) \left(-g^{\beta\beta'} \right) = \frac{1}{2} \left(-g^{\alpha\beta} + \frac{k^\alpha K^\beta}{k \cdot K} \right), \quad (2.24)$$

one can obtain the helicity amplitude

$$H_{QCD}^q = T^{\alpha\beta} \mathbb{P}_{\alpha\beta} = \frac{2Q_c}{3\sqrt{3}} \sqrt{4\pi\alpha} (4\pi\alpha_s)^2 \sum_{q=u,d,s} f_{\eta^{(r)}}^q H_q, \quad (2.25)$$

where the dimensionless function H_q reads

$$H_q = -8i \int \frac{d^3q}{(2\pi)^3} f(\hat{q}^2) \int du \phi^q(u) I_q(u, \hat{q}). \quad (2.26)$$

$I_q(u, \hat{q})$ represents the sum of the loop integrals of all the Feynman diagrams

$$\begin{aligned} I_q(u, \hat{q}) = \int \frac{d^4l}{(2\pi)^4} & \left(\frac{N_1}{D_1 D_2 D_3 D_4 D_5} + \frac{N_2}{D_1 D'_2 D'_3 D_4 D_5} + \frac{N_3}{C_1 D_1 D_3 D_4 D_5} \right. \\ & \left. + \frac{N_4}{C_2 D_1 D_2 D_4 D_5} + \frac{N_5}{C_1 D_1 D'_2 D_4 D_5} + \frac{N_6}{C_2 D_1 D'_3 D_4 D_5} \right) + (u \leftrightarrow \bar{u}) \end{aligned} \quad (2.27)$$

with $l = k_1 - k_2$ and the denominators of the propagators

$$C_1 = (p - k + 2\hat{q})^2 - 4m_c^2 + i\epsilon,$$

$$\begin{aligned}
C_2 &= (p - k - 2\hat{q})^2 - 4m_c^2 + i\epsilon, \\
D_1 &= [l + (\bar{u} - u)p]^2 - 4m_q^2 + i\epsilon, \\
D_2 &= (l - k - 2\hat{q})^2 - 4m_c^2 + i\epsilon, \\
D_3 &= (l + k - 2\hat{q})^2 - 4m_c^2 + i\epsilon, \\
D'_2 &= (l - k + 2\hat{q})^2 - 4m_c^2 + i\epsilon, \\
D'_3 &= (l + k + 2\hat{q})^2 - 4m_c^2 + i\epsilon, \\
D_4 &= (l + p)^2 + i\epsilon, \\
D_5 &= (l - p)^2 + i\epsilon.
\end{aligned} \tag{2.28}$$

As shown in Eq. (2.26), the spin structures of the bound state wave function are absorbed into the numerators N_1, N_2, N_3, N_4, N_5 and N_6 . And the expressions of the numerators are presented in appendix A. Since the loop function $I_q(u, \hat{q})$ has no soft singularities and the dimensionless function H_q is very insensitive to the light quark mass m_q [18, 27], one can take the following simplicity safely:

$$\begin{aligned}
I_0(u, \hat{q}) &= \lim_{m_q \rightarrow 0} I_q(u, \hat{q}), \\
H_0 &= -8i \int \frac{d^3 \hat{q}}{(2\pi)^3} f(\hat{q}^2) \int du \phi^q(u) I_0(u, \hat{q}),
\end{aligned} \tag{2.29}$$

i.e., $H_q(q = u, d, s) = H_0$. Then the helicity amplitude in Eq. (2.25) can be rewritten as

$$H_{QCD}^q = \frac{2Q_c}{3\sqrt{3}} \sqrt{4\pi\alpha} (4\pi\alpha_s)^2 f_{\eta^{(\prime)}} H_0 \tag{2.30}$$

with the effective decay constants

$$f_{\eta'} = f_{\eta'}^u + f_{\eta'}^d + f_{\eta'}^s, \quad f_{\eta} = f_{\eta}^u + f_{\eta}^d + f_{\eta}^s. \tag{2.31}$$

By using the algebraic identity ($\xi \neq \pm 1$)

$$\frac{1}{m^2(\xi^2 - 1)} D_1 - \frac{1}{2m^2(\xi - 1)} D_4 + \frac{1}{2m^2(\xi + 1)} D_5 = 1 \tag{2.32}$$

with $\xi = 1 - 2u$, the loop integral $I_0(u, \hat{q})$ can be decomposed into a sum of four-point one-loop integrals

$$\begin{aligned}
I_0(u, \hat{q}) = & \int \frac{d^4 l}{(2\pi)^4} \left[\frac{1}{m^2} \left(\frac{N_1}{(\xi^2 - 1)D_2 D_3 D_4 D_5} - \frac{N_1}{2(\xi - 1)D_1 D_2 D_3 D_5} + \frac{N_1}{2(\xi + 1)D_1 D_2 D_3 D_4} \right. \right. \\
& + \frac{N_2}{(\xi^2 - 1)D'_2 D'_3 D_4 D_5} - \frac{N_2}{2(\xi - 1)D_1 D'_2 D'_3 D_5} + \frac{N_2}{2(\xi + 1)D_1 D'_2 D'_3 D_4} \left. \right) + \frac{N_3}{C_1 D_1 D_3 D_4 D_5} \\
& \left. + \frac{N_4}{C_2 D_1 D_2 D_4 D_5} + \frac{N_5}{C_1 D_1 D'_2 D_4 D_5} + \frac{N_6}{C_2 D_1 D'_3 D_4 D_5} \right] + (u \leftrightarrow \bar{u}). \tag{2.33}
\end{aligned}$$

When $\xi = 1$, the denominators of the propagators have the relation $D_1 = D_4$, and the loop integral $I_0(u, \hat{q})$ becomes

$$\begin{aligned}
I_0(u, \hat{q}) = & \int \frac{d^4 l}{(2\pi)^4} \left(\frac{N_1}{D_2 D_3 D_4^2 D_5} + \frac{N_2}{D'_2 D'_3 D_4^2 D_5} + \frac{N_3}{C_1 D_3 D_4^2 D_5} \right. \\
& \left. + \frac{N_4}{C_2 D_2 D_4^2 D_5} + \frac{N_5}{C_1 D'_2 D_4^2 D_5} + \frac{N_6}{C_2 D'_3 D_4^2 D_5} \right) + (u \leftrightarrow \bar{u}). \tag{2.34}
\end{aligned}$$

And when $\xi = -1$, the denominators of the propagators have the relation $D_1 = D_5$, and the loop integral $I_0(u, \hat{q})$ becomes

$$\begin{aligned}
I_0(u, \hat{q}) = & \int \frac{d^4 l}{(2\pi)^4} \left(\frac{N_1}{D_2 D_3 D_4 D_5^2} + \frac{N_2}{D'_2 D'_3 D_4 D_5^2} + \frac{N_3}{C_1 D_3 D_4 D_5^2} \right. \\
& \left. + \frac{N_4}{C_2 D_2 D_4 D_5^2} + \frac{N_5}{C_1 D'_2 D_4 D_5^2} + \frac{N_6}{C_2 D'_3 D_4 D_5^2} \right) + (u \leftrightarrow \bar{u}). \tag{2.35}
\end{aligned}$$

With the program *Package - X* [61, 62], one can evaluate the above one-loop integrals analytically. Similar to the situations without considering the internal momentum [18, 27], one can find that the loop function $I_0(u, \hat{q})$ is also steady over the most region of the momentum fraction u , and it results in the dimensionless function H_0 very insensitive to the shapes of meson DAs $\phi^q(u)$. Numerically, our results show that the change among the dimensionless function H_0 with the different models of the DAs in Fig. 2 is less than 1%.

2.3 The contributions of the gluonic content of $\eta^{(\prime)}$

The gluonic content of $\eta^{(\prime)}$ can directly contribute to the decay processes $h_c \rightarrow \gamma \eta^{(\prime)}$ from the tree level. One typical Feynman diagram is exhibited in Fig. 3, and there are other two diagrams from permutations of the photon and the gluon legs.

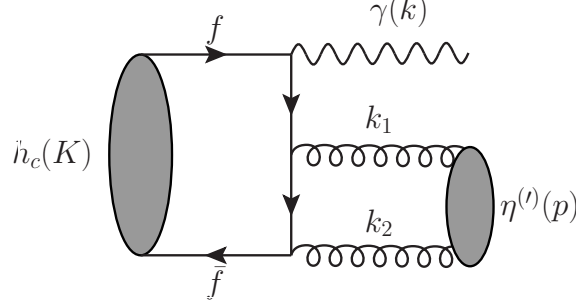


Figure 3: One typical Feynman diagram for $h_c \rightarrow \gamma \eta^{(\prime)}$ with the gluonic content of $\eta^{(\prime)}$. Here the kinematical variables are labeled.

The matrix elements of the mesons $\eta^{(\prime)}$ over two-gluon fields in the light-cone expansion at the leading twist level read [56, 60, 63]:

$$\langle \eta^{(\prime)}(p) | A_\alpha^a(x) A_\beta^b(y) | 0 \rangle = \frac{1}{4} \epsilon_{\alpha\beta\mu\nu} \frac{k^\mu p^\nu}{p \cdot k} \frac{C_F}{\sqrt{3}} \frac{\delta^{ab}}{8} f_{\eta^{(\prime)}}^1 \int du e^{i(u p \cdot x + \bar{u} p \cdot y)} \frac{\phi^g(u)}{u(1-u)} \quad (2.36)$$

with the effective decay constant $f_{\eta^{(\prime)}}^1 = \frac{1}{\sqrt{3}}(f_{\eta^{(\prime)}}^u + f_{\eta^{(\prime)}}^d + f_{\eta^{(\prime)}}^s)$ and the gluonic twist-2 DA [56, 60, 64]

$$\phi^g(u) = 30u^2(1-u)^2 \sum_{n=2,4,\dots} c_n^g(\mu) C_{n-1}^{\frac{5}{2}}(2u-1). \quad (2.37)$$

One can obtain the corresponding helicity amplitude

$$H_{QCD}^g = \frac{2Q_c}{9} \sqrt{4\pi\alpha} (4\pi\alpha_s) f_{\eta^{(\prime)}}^1 H_g, \quad (2.38)$$

where the dimensionless function H_g has the form

$$H_g = 8 \int \frac{d^3\hat{q}}{(2\pi)^3} f(\hat{q}^2) \int du \frac{\phi^g(u)}{u(1-u)} \left(\frac{N_7}{C_1 C_4} + \frac{N_8}{C_2 C_3} + \frac{N_9}{C_3 C_4} \right). \quad (2.39)$$

Here the denominators of the propagators C_3 and C_4 read

$$\begin{aligned} C_3 &= (\xi p + k + 2\hat{q})^2 - 4m_c^2 + i\epsilon, \\ C_4 &= (\xi p - k + 2\hat{q})^2 - 4m_c^2 + i\epsilon, \end{aligned} \quad (2.40)$$

and the expressions of the numerators N_7 , N_8 and N_9 are given in appendix A.

Usually, from the point of view of the QCD evolution of the gluon DA, the contributions of the gluonic content are supposed to be small, since the gluonic content is seen as the higher-order effects. However, as we have pointed out in Ref. [27], these contributions may become important in the $\eta^{(\prime)}$ production since the two-gluon DA of $\eta^{(\prime)}$ can mix with their quark-antiquark DA due to the $U_A(1)$ anomaly. Furthermore, from Figs. 1 and 3, one can easily find that the one-loop contributions from the quark-antiquark content of $\eta^{(\prime)}$ are suppressed by a factor of $\alpha_s(m_c)$ as compared with the contributions from the gluonic content of $\eta^{(\prime)}$.

3 Numerical results

The decay widths of $h_c \rightarrow \gamma \eta^{(\prime)}$ can be expressed as

$$\Gamma(h_c \rightarrow \gamma \eta^{(\prime)}) = \frac{2}{3} \frac{1-x}{16\pi M} |H_{QCD}^q + H_{QCD}^g|^2 \quad (3.1)$$

with $x = m^2/M^2$. In the following numerical calculations, we take the parameters: $M = 3525$ MeV, $m_\eta = 548$ MeV, $m_{\eta'} = 958$ MeV, $\Gamma_{h_c} = (0.70 \pm 0.28 \pm 0.22)$ MeV and $f_\pi = 130.2$ MeV, which are quoted from the PDG [65]. The input c -quark mass is taken as $m_c = 1490$ MeV, which is chosen from the calculation of the mass spectrum of charmonium [43, 44]. The harmonic oscillator parameter, which characterize the typical internal momentum of a bound state, is taken as $\beta_A = 590$ MeV for the P -wave charmonium h_c [43, 44][†]. The QCD

[†]In Refs. [43, 44], the harmonic oscillator parameter β_A is expressed as

$$\beta_A = \left(-\frac{m_c \omega_{q\bar{q}}^2 \Theta_A}{\sqrt{1 + 2A_0(N + \frac{3}{2})}} \right)^{\frac{1}{4}}.$$

For the axial vector meson h_c , $\Theta_A = -4$, $N = 1$, the potential parameters $\omega_{q\bar{q}}^2 = 2.084 \times 10^7$ MeV³ and $A_0 = 0.01$.

running coupling constant is adopted $\alpha_s(\mu) = 0.35$, which is calculated through the two-loop renormalization group equation at the scale of $\mu = m_c$.

As shown in Table 1, the Gegenbauer moments $c_2^q(\mu)$, $c_4^q(\mu)$ have large uncertainties. Fortunately, the dimensionless function H_q is very insensitive to the shape of the meson DA, which means our numerical results are almost independent to the uncertainties of the Gegenbauer moments $c_2^q(\mu)$, $c_4^q(\mu)$. So in our calculations, we could choose the Model I of the meson DA in Table 1.

For $\eta - \eta'$ system, one mixing angle is included in the flavor basis as a manifestation of the celebrated OZI rule, i.e., we take the known FKS scheme [19, 66, 67], and more details can also be found in Ref. [60]. Then the effective decay constants $f_{\eta^{(\prime)}}^q$ can be expressed as

$$\begin{aligned} f_{\eta}^{u(d)} &= \frac{f_q}{\sqrt{2}} \cos \phi, & f_{\eta}^s &= -f_s \sin \phi, \\ f_{\eta'}^{u(d)} &= \frac{f_q}{\sqrt{2}} \sin \phi, & f_{\eta'}^s &= f_s \cos \phi, \end{aligned} \quad (3.2)$$

where the two parameters f_q and f_s are defined as [19, 66, 67]

$$\begin{aligned} \langle 0 | J_{\mu 5}^q(0) | \eta_q(p) \rangle &= i f_q p_{\mu}, & \langle 0 | J_{\mu 5}^q(0) | \eta_s(p) \rangle &= 0, \\ \langle 0 | J_{\mu 5}^s(0) | \eta_s(p) \rangle &= i f_s p_{\mu}, & \langle 0 | J_{\mu 5}^s(0) | \eta_q(p) \rangle &= 0 \end{aligned} \quad (3.3)$$

with the currents $J_{\mu 5}^q = 1/\sqrt{2}(\bar{u}\gamma_{\mu}\gamma_5 u + \bar{d}\gamma_{\mu}\gamma_5 d)$ and $J_{\mu 5}^s = \bar{s}\gamma_{\mu}\gamma_5 s$. In the literature, the mixing angle ϕ and the decay constants f_q and f_s have been determined by various methods [19, 68–73]. In Table 2, we list three typical sets of the values of the parameters ϕ , f_q and f_s from Refs. [68, 72]. The parameters ϕ , f_q and f_s in the first line are extracted from the low energy processes (LEPs) $V \rightarrow \eta^{(\prime)}\gamma$, $\eta^{(\prime)} \rightarrow V\gamma$ ($V = \rho, \omega, \phi$). The parameters in the second line are extracted by using rational approximations for the η TFF $F_{\gamma^*\gamma\eta}(Q^2 \rightarrow +\infty)$. And the obtained parameters both in the first and second lines are consistent with the known FKS results [19]. While in the third line, the parameters are extracted by using rational approximations for the η' TFF $F_{\gamma^*\gamma\eta'}(Q^2 \rightarrow +\infty)$, which is in accord with the BABAR measurements in the timelike region at $q^2 = 112 \text{ GeV}^2$ [74].

In Table 3, we present the results with only the contributions of the quark-antiquark content.

Table 2: The values of ϕ , f_q and f_s obtained with three different models.

	ϕ°	f_q/f_π	f_s/f_π
LEPs [68]	40.6 ± 0.9	1.10 ± 0.03	1.66 ± 0.06
η TFF [72]	40.3 ± 1.8	1.06 ± 0.01	1.56 ± 0.24
η' TFF [72]	33.5 ± 0.9	1.09 ± 0.02	0.96 ± 0.04

Table 3: The branching ratios $\mathcal{B}(h_c \rightarrow \gamma\eta^{(\prime)})$ with only the contributions of the quark-antiquark content.

	LEPs	η TFF	η' TFF	Exp. [9]
$\mathcal{B}(h_c \rightarrow \gamma\eta)$	1.4×10^{-6}	2.4×10^{-6}	0.8×10^{-4}	$(4.7 \pm 1.5 \pm 1.4) \times 10^{-4}$
$\mathcal{B}(h_c \rightarrow \gamma\eta')$	0.47×10^{-3}	0.43×10^{-3}	0.25×10^{-3}	$(1.52 \pm 0.27 \pm 0.29) \times 10^{-3}$
R_{h_c}	0.3%	0.6%	30.2%	$(30.7 \pm 11.3 \pm 8.7)\%$

The branching ratios $\mathcal{B}(h_c \rightarrow \gamma\eta)$, $\mathcal{B}(h_c \rightarrow \gamma\eta')$ and their ratio $R_{h_c} = \mathcal{B}(h_c \rightarrow \gamma\eta)/\mathcal{B}(h_c \rightarrow \gamma\eta')$ are given in the first, second and third lines of the tables with $\Gamma_{h_c} = 0.70$ MeV, respectively. From Table 3, one can find that the branching ratio $\mathcal{B}(h_c \rightarrow \gamma\eta)$ is sensitive to the mixing angle, and the results of $\mathcal{B}(h_c \rightarrow \gamma\eta)$ with the parameters extracted from the LEPs and η TFF are much smaller than its experimental data. Only with the values in the set η' TFF, both the branching ratios $\mathcal{B}(h_c \rightarrow \gamma\eta)$ and $\mathcal{B}(h_c \rightarrow \gamma\eta')$ are comparable with their experimental values. In fact, due to the large uncertainty of the total decay width Γ_{h_c} , it is very hard to give precise predictions for individual branching ratios. While in the ratio R_{h_c} , this uncertainty cancel out. This means the R_{h_c} could be reliably predicted and one can find that the R_{h_c} only with the parameters extracted from the η' TFF is in good agreement with the experimental data.

Table 4: The branching ratios $\mathcal{B}(h_c \rightarrow \gamma\eta^{(\prime)})$ with the contributions of both the quark-antiquark content and the gluonic content.

	LEPs	η TFF	η' TFF	Exp. [9]
$\mathcal{B}(h_c \rightarrow \gamma\eta)$	2.9×10^{-6}	5.1×10^{-6}	1.6×10^{-4}	$(4.7 \pm 1.5 \pm 1.4) \times 10^{-4}$
$\mathcal{B}(h_c \rightarrow \gamma\eta')$	0.99×10^{-3}	0.89×10^{-3}	0.52×10^{-3}	$(1.52 \pm 0.27 \pm 0.29) \times 10^{-3}$
R_{h_c}	0.3%	0.6%	30.9%	$(30.7 \pm 11.3 \pm 8.7)\%$

Considering the contributions of both the quark-antiquark content and the gluonic content, the branching ratios with $\Gamma_{h_c} = 0.70$ MeV and the ratio R_{h_c} are given in Table 4. Compared to Table 3, one can find that the branching ratios $\mathcal{B}(h_c \rightarrow \gamma\eta^{(\prime)})$ are enhanced by a factor of about 2 with no matter which set of the values is taken, i.e., the gluonic content is almost

Table 5: The branching ratios obtained with the zero-binding approximation and the B-S equation under CIA.

	$ R'_{h_c}(0) $ [27]	this work	Exp. [9]
$\mathcal{B}(h_c \rightarrow \gamma\eta)$	1.1×10^{-4}	1.6×10^{-4}	$(4.7 \pm 1.5 \pm 1.4) \times 10^{-4}$
$\mathcal{B}(h_c \rightarrow \gamma\eta')$	0.37×10^{-3}	0.52×10^{-3}	$(1.52 \pm 0.27 \pm 0.29) \times 10^{-3}$
R_{h_c}	30.1%	30.9%	$(30.7 \pm 11.3 \pm 8.7)\%$

as important as the quark-antiquark content in the P -wave charmonium decays $h_c \rightarrow \gamma\eta^{(\prime)}$. The agreement between our prediction and the experimental measurement for the ratio R_{h_c} is good only with the parameters extracted from η' TFF. In Table 5, we make a comparison between the results with the zero-binding approximation [27] and these with the B-S equation under CIA. One can find that the R_{h_c} is almost unchanged. Furthermore, for the individual branching ratios with the zero-binding approximation [27] and the ones with the B-S equation under CIA, one can obtain that their difference comes mainly from the QCD running coupling constant $\alpha_s(\mu)$ in fact[†], i.e., the relativistic corrections related to the internal momentum \hat{q} are almost negligible. It implies that the nonrelativistic limit for the P -wave charmonium h_c , in which the Taylor expansion of the hard kernels is kept up to the linear terms, may be a good approximation for the radiative decays $h_c \rightarrow \gamma\eta^{(\prime)}$.

As a crossing check, we give a prediction of the mixing angle ϕ within the B-S equation approach. By the ratio

$$R_{h_c} = \frac{M^2 - m_\eta^2}{M^2 - m_{\eta'}^2} \frac{|H_{QCD}^q + H_{QCD}^g|_{m=m_\eta}^2}{|H_{QCD}^q + H_{QCD}^g|_{m=m_{\eta'}}^2}, \quad (3.4)$$

the ratio

$$\frac{\Gamma(\eta \rightarrow \gamma\gamma)}{\Gamma(\eta' \rightarrow \gamma\gamma)} = \frac{m_\eta^3}{m_{\eta'}^3} \left(\frac{5\sqrt{2}\frac{f_s}{f_q} - 2\tan\phi}{5\sqrt{2}\frac{f_s}{f_q}\tan\phi + 2} \right)^2 \quad (3.5)$$

and the experimental measurements [9, 65, 75]

$$R_{h_c}^{exp} = (30.7 \pm 11.3 \pm 8.7)\%,$$

[†]In Ref. [27], we take the QCD running coupling constant $\alpha_s(\mu) = 0.32$ with the scale of $\mu = M/2 = 3525/2$ MeV. While in this work, the QCD running coupling constant is taken as $\alpha_s(\mu) = 0.35$ with the scale of $\mu = m_c = 1490$ MeV.

$$\begin{aligned}
\Gamma^{exp}(\eta' \rightarrow \gamma\gamma) &= 4.36(14) \text{ KeV}, \\
\Gamma^{exp}(\eta \rightarrow \gamma\gamma) &= 0.516(18) \text{ KeV},
\end{aligned}
\tag{3.6}$$

one can obtain the mixing angle

$$\phi = 33.8^\circ \pm 2.4^\circ, \tag{3.7}$$

where the uncertainty comes mainly from the $R_{h_c}^{exp}$. It is worth noting that the recent QCD lattice calculations give the following values: $\phi = 34^\circ \pm 3^\circ$ from the UKQCD collaboration [70] and $\phi = 38.8^\circ \pm 3.3^\circ$ from the ETM collaboration [73]. In Fig. 4, we show the dependence

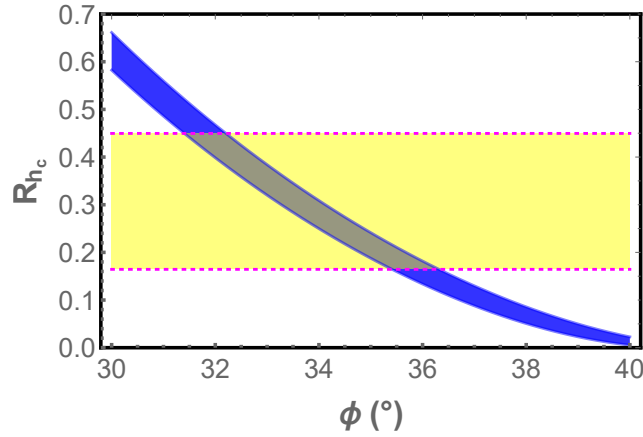


Figure 4: The dependence of the ratio R_{h_c} on the mixing angle ϕ . The blue band is our calculated results with the uncertainties from the $\Gamma^{exp}(\eta^{(\prime)} \rightarrow \gamma\gamma)$. The yellow band denotes the experimental value of R_{h_c} with 1σ uncertainty.

of the ratio R_{h_c} on the mixing angle ϕ . Obviously, the prediction of the mixing angle with the B-S equation under CIA is consistent with the value $\phi = 33.5^\circ \pm 0.9^\circ$ in the set η' TFF. Moreover, it is also in good agreement with our previous determinations $\phi = 33.9^\circ \pm 0.6^\circ$ [18] and $\phi = 33.8^\circ \pm 2.5^\circ$ [27], which are obtained by the ratios $R_{J/\psi}$ and R_{h_c} without considering the relativistic corrections related to the internal momentum of J/ψ and h_c respectively. And this agreement is in line with the conclusion obtained from Table 5, i.e., the relativistic corrections related to the internal momentum \hat{q} are almost negligible to the P -wave charmonium decays $h_c \rightarrow \gamma\eta^{(\prime)}$ within the B-S equation approach. However, there is discrepancy between our predictions and the result $\phi = 40.6^\circ \pm 0.9^\circ$ in the set of LEPs extracted from the LEPs [68]. As we have pointed out in Refs. [18, 27], this discrepancy may be partly due to the $g^*g^* - \eta^{(\prime)}$ TFF

used in our calculations and may also be an indication of our incomplete knowledge about the $\eta - \eta'$ mixing, especially the difference between the physical picture of the $\eta - \eta'$ mixing at the high energy scale and that at the low energy scale [76].

4 Summary

In this work, we have revisited the P -wave charmonium radiative decays $h_c \rightarrow \gamma\eta^{(\prime)}$ in the B-S equation framework, where the internal momentum \hat{q} has been retained in both the soft wave function $\psi(\hat{q})$ and the hard kernel $\mathcal{O}(\hat{q})$. The B-S wave function with CIA is employed to describe the bound state properties of the P -wave charmonium h_c , while the light-cone DAs are adopted for both the quark-antiquark content and the gluonic content of the light mesons $\eta^{(\prime)}$. With the technique of the helicity projector [11], the involved one-loop integrals are carried out analytically. Then it is found that the branching ratios $\mathcal{B}(h_c \rightarrow \gamma\eta^{(\prime)})$ are insensitive to the light quark masses and the shapes of the $\eta^{(\prime)}$ DAs.

With the three sets of the values for the input parameters ϕ , f_q and f_s , namely LEPs [68], η TFF [72] and η' TFF [72], the predicted branching ratios $\mathcal{B}(h_c \rightarrow \gamma\eta^{(\prime)})$ and their ratio R_{h_c} are presented in Table 3 and 4. We have found that the gluonic content also plays an important role in $h_c \rightarrow \gamma\eta^{(\prime)}$, and the $\mathcal{B}(h_c \rightarrow \gamma\eta)$ with the parameters extracted from the LEPs and the η TFF is much smaller than its experimental value. Only with the parameters extracted from η' TFF, which is in accord with the BABAR measurements in the timelike region at $q^2 = 112 \text{ GeV}^2$ [74], the branching ratios $\mathcal{B}(h_c \rightarrow \gamma\eta^{(\prime)})$ and the ratio R_{h_c} are comparable with their experimental values. In addition, by the comparison between the results with the zero-binding approximation [27] and these obtained in this work, one can obtain that the relativistic corrections related to the internal momentum \hat{q} are almost negligible in the P -wave charmonium decays $h_c \rightarrow \gamma\eta^{(\prime)}$ in the B-S equation framework.

As a crossing check, by the R_{h_c} , $\Gamma(\eta^{(\prime)} \rightarrow \gamma\gamma)$ and their experimental values, we have obtained the mixing angle $\phi = 33.8^\circ \pm 2.4^\circ$, which is consistent with the our previous determinations $\phi = 33.9^\circ \pm 0.6^\circ$ [18] and $\phi = 33.8^\circ \pm 2.5^\circ$ [27] by the ratios $R_{J/\psi}$ and R_{h_c} obtained with zero-binding approximation in the nonrelativistic limit respectively, but is in clear disagreement with the value $\phi = 40.6^\circ \pm 0.9^\circ$ [68] extracted from the LEPs and the known FKS result

$\phi = 39.3^\circ \pm 1.0^\circ$ [19]. As aforementioned discussion, the discrepancy among the determinations of the mixing angle is still an open question, and it indicates that the physical picture of the $\eta - \eta'$ mixing at the high energy scale may differ from that at the low energy scale [76]. Further investigations about this issue is certainly deserved.

Acknowledgements

This work is supported by the National Natural Science Foundation of China under Grant Nos. 11675061, 11775092 and 11435003.

A The expressions of the numerators

The expressions of the numerators N_i ($i = 1 \sim 9$) read

$$\begin{aligned}
N_1 &= 4M^2m_c(x-1)\hat{q} \cdot l + M(x+1) \left[\hat{q} \cdot l(4m_c^2 + 4\hat{q} \cdot l + l^2) - 4\hat{q}^2(\hat{q} \cdot l + l^2) \right] \\
&\quad + 8m_ck \cdot \hat{q} \left[\frac{x+1}{x-1}k \cdot l + p \cdot l \right] + \frac{2K \cdot l}{M} \left\{ k \cdot \hat{q} \left[4m_c^2 - 4\hat{q}^2 + 4\hat{q} \cdot l + \frac{x+3}{x-1}l^2 \right] \right. \\
&\quad \left. + 2p \cdot l(2\hat{q}^2 - \hat{q} \cdot l) \right\} - \frac{8k \cdot \hat{q}p \cdot l(K \cdot l)^2}{M^3(x-1)} \\
N_2 &= -4M^2m_c(x-1)\hat{q} \cdot l - M(x+1) \left[\hat{q} \cdot l(4m_c^2 + l^2 - 4\hat{q} \cdot l) - 4\hat{q}^2(\hat{q} \cdot l - l^2) \right] \\
&\quad - 8m_ck \cdot \hat{q} \left[\frac{x+1}{x-1}k \cdot l + p \cdot l \right] - \frac{2K \cdot l}{M} \left\{ k \cdot \hat{q} \left[4m_c^2 - 4\hat{q}^2 - 4\hat{q} \cdot l + \frac{x+3}{x-1}l^2 \right] \right. \\
&\quad \left. - 2p \cdot l(2\hat{q}^2 + \hat{q} \cdot l) \right\} + \frac{8k \cdot \hat{q}p \cdot l(K \cdot l)^2}{M^3(x-1)} \\
N_3 &= M^2x \left[M(x-1) + 4m_c \right] \hat{q} \cdot l + 2M \left\{ k \cdot \hat{q} \left[\frac{x(x-3)}{x-1}k \cdot l + (x-2)p \cdot l - 2(x+1)\hat{q} \cdot l \right. \right. \\
&\quad \left. \left. - \frac{2x}{x-1}l^2 \right] - \left[2m_c^2(x+1)\hat{q} \cdot l - 2(x+1)\hat{q}^2(\hat{q} \cdot l - l^2) + xp \cdot l\hat{q} \cdot l \right] \right\} + 4m_c \left\{ 2k \cdot \hat{q} \right. \\
&\quad \left. \times \left[\frac{x}{x-1}k \cdot l + p \cdot l - \frac{1}{x-1}l^2 \right] + p \cdot l\hat{q} \cdot l \right\} - \frac{4}{M} \left\{ 2k \cdot \hat{q}K \cdot l(m_c^2 + k \cdot \hat{q}) - 2k \cdot \hat{q}\hat{q}^2K \cdot l \right. \\
&\quad \left. + k \cdot \hat{q}p \cdot l \left[\frac{x}{x-1}k \cdot l + \frac{x-2}{x-1}p \cdot l \right] - 2\hat{q}^2p \cdot lK \cdot l \right\} + \frac{8m_ck \cdot \hat{q}p \cdot lK \cdot l}{M^2(x-1)} \\
N_4 &= M^2x \left[M(x-1) + 4m_c \right] \hat{q} \cdot l + 2M \left\{ k \cdot \hat{q} \left[\frac{x(x-3)}{x-1}k \cdot l + (x-2)p \cdot l + 2(x+1)\hat{q} \cdot l \right. \right.
\end{aligned}$$

$$\begin{aligned}
& + \frac{2x}{x-1} l^2 \Big] - \left[2m_c^2(x+1) \hat{q} \cdot l - 2(x+1) \hat{q}^2 (\hat{q} \cdot l - l^2) - xp \cdot l \hat{q} \cdot l \right] \Big\} + 4m_c \left\{ 2k \cdot \hat{q} \right. \\
& \times \left[\frac{x}{x-1} k \cdot l + p \cdot l + \frac{1}{x-1} l^2 \right] - p \cdot l \hat{q} \cdot l \Big\} - \frac{4}{M} \left\{ 2k \cdot \hat{q} K \cdot l (m_c^2 - k \cdot \hat{q}) - 2k \cdot \hat{q} \hat{q}^2 K \cdot l \right. \\
& \left. - k \cdot \hat{q} p \cdot l \left[\frac{x}{x-1} k \cdot l + \frac{x-2}{x-1} p \cdot l \right] - 2\hat{q}^2 p \cdot l K \cdot l \right\} - \frac{8m_c k \cdot \hat{q} p \cdot l K \cdot l}{M^2(x-1)} \\
N_5 = & -M^2 x \left[M(x-1) + 4m_c \right] \hat{q} \cdot l - 2M \left\{ k \cdot \hat{q} \left[\frac{x(x-3)}{x-1} k \cdot l + (x-2) p \cdot l - 2(x+1) \hat{q} \cdot l \right. \right. \\
& \left. \left. + \frac{2x}{x-1} l^2 \right] - \left[2m_c^2(x+1) \hat{q} \cdot l - 2(x+1) \hat{q}^2 (\hat{q} \cdot l + l^2) - xp \cdot l \hat{q} \cdot l \right] \right\} - 4m_c \left\{ 2k \cdot \hat{q} \right. \\
& \times \left[\frac{x}{x-1} k \cdot l + p \cdot l + \frac{1}{x-1} l^2 \right] - p \cdot l \hat{q} \cdot l \Big\} + \frac{4}{M} \left\{ 2k \cdot \hat{q} K \cdot l (m_c^2 + k \cdot \hat{q}) - 2k \cdot \hat{q} \hat{q}^2 K \cdot l \right. \\
& \left. - k \cdot \hat{q} p \cdot l \left[\frac{x}{x-1} k \cdot l + \frac{x-2}{x-1} p \cdot l \right] + 2\hat{q}^2 p \cdot l K \cdot l \right\} + \frac{8m_c k \cdot \hat{q} p \cdot l K \cdot l}{M^2(x-1)} \\
N_6 = & -M^2 x \left[M(x-1) + 4m_c \right] \hat{q} \cdot l - 2M \left\{ k \cdot \hat{q} \left[\frac{x(x-3)}{x-1} k \cdot l + (x-2) p \cdot l + 2(x+1) \hat{q} \cdot l \right. \right. \\
& \left. \left. - \frac{2x}{x-1} l^2 \right] - \left[2m_c^2(x+1) \hat{q} \cdot l - 2(x+1) \hat{q}^2 (\hat{q} \cdot l + l^2) + xp \cdot l \hat{q} \cdot l \right] \right\} - 4m_c \left\{ 2k \cdot \hat{q} \right. \\
& \times \left[\frac{x}{x-1} k \cdot l + p \cdot l - \frac{1}{x-1} l^2 \right] + p \cdot l \hat{q} \cdot l \Big\} + \frac{4}{M} \left\{ 2k \cdot \hat{q} K \cdot l (m_c^2 - k \cdot \hat{q}) - 2k \cdot \hat{q} \hat{q}^2 K \cdot l \right. \\
& \left. + k \cdot \hat{q} p \cdot l \left[\frac{x}{x-1} k \cdot l + \frac{x-2}{x-1} p \cdot l \right] + 2\hat{q}^2 p \cdot l K \cdot l \right\} - \frac{8m_c k \cdot \hat{q} p \cdot l K \cdot l}{M^2(x-1)} \\
N_7 = & \frac{M(x\xi + x - 1) - 2m_c(\xi - 1)}{x-1} k \cdot \hat{q} + M(x-1) \xi \hat{q}^2 - \frac{4k \cdot \hat{q}}{M(x-1)} \left(m_c^2 + k \cdot \hat{q} - \hat{q}^2 \right) \\
N_8 = & \frac{M(-x\xi + x - 1) + 2m_c(\xi + 1)}{x-1} k \cdot \hat{q} + M(x-1) \xi \hat{q}^2 - \frac{4k \cdot \hat{q}}{M(x-1)} \left(m_c^2 - k \cdot \hat{q} - \hat{q}^2 \right) \\
N_9 = & \frac{4m_c^2 - M^2 \xi^2}{M(x-1)} k \cdot \hat{q} + M(x-1) \xi \hat{q}^2 + \frac{4k \cdot \hat{q}}{M(x-1)} \left(\xi k \cdot \hat{q} - \hat{q}^2 \right). \tag{A.1}
\end{aligned}$$

References

- [1] **E598** Collaboration, J. J. Aubert et al., *Experimental Observation of a Heavy Particle J*, *Phys. Rev. Lett.* **33** (1974) 1404.
- [2] **SLAC-SP-017** Collaboration, J. E. Augustin et al., *Discovery of a Narrow Resonance in e^+e^- Annihilation*, *Phys. Rev. Lett.* **33** (1974) 1406. [Adv. Exp. Phys.5,141(1976)].
- [3] **BES** Collaboration, M. Ablikim et al., *Measurement of the branching fractions for $J/\psi \rightarrow \gamma\pi^0$, $\gamma\eta$ and $\gamma\eta'$* , *Phys. Rev.* **D73** (2006) 052008, [hep-ex/0510066].

- [4] **CLEO** Collaboration, J. Libby et al., *Measurement of the η' -meson mass using $J/\psi \rightarrow \gamma\eta'$* , *Phys. Rev. Lett.* **101** (2008) 182002, [[arXiv:0806.2344](#)].
- [5] **CLEO** Collaboration, T. K. Pedlar et al., *Charmonium decays to $\gamma\pi^0$, $\gamma\eta$ and $\gamma\eta'$* , *Phys. Rev.* **D79** (2009) 111101, [[arXiv:0904.1394](#)].
- [6] **BESIII** Collaboration, M. Ablikim et al., *Measurement of the Matrix Element for the Decay $\eta' \rightarrow \eta\pi^+\pi^-$* , *Phys. Rev.* **D83** (2011) 012003, [[arXiv:1012.1117](#)].
- [7] **BESIII** Collaboration, M. Ablikim et al., *Evidence for ψ' decays into $\gamma\pi^0$ and $\gamma\eta$* , *Phys. Rev. Lett.* **105** (2010) 261801, [[arXiv:1011.0885](#)].
- [8] **BESIII** Collaboration, M. Ablikim et al., *Measurement of branching fractions for $\psi(3686) \rightarrow \gamma\eta', \gamma\eta$ and $\gamma\pi^0$* , *Phys. Rev.* **D96** (2017) 052003, [[arXiv:1708.03103](#)].
- [9] **BESIII** Collaboration, M. Ablikim et al., *Observation of h_c radiative decay $h_c \rightarrow \gamma\eta'$ and evidence for $h_c \rightarrow \gamma\eta$* , *Phys. Rev. Lett.* **116** (2016) 251802, [[arXiv:1603.04936](#)].
- [10] V. A. Novikov, M. A. Shifman, A. I. Vainshtein, and V. I. Zakharov, *A Theory of the $J/\psi \rightarrow \eta(\eta')\gamma$ Decays*, *Nucl. Phys.* **B165** (1980) 55.
- [11] J. G. Körner, J. H. Kühn, M. Krammer, and H. Schneider, *Zweig Forbidden Radiative Orthoquarkonium Decays in Perturbative QCD*, *Nucl. Phys.* **B229** (1983) 115.
- [12] K.-T. Chao, *Issue of $\psi \rightarrow \gamma\eta, \gamma\eta'$ Decays and $\eta - \eta'$ Mixing*, *Phys. Rev.* **D39** (1989) 1353.
- [13] K.-T. Chao, *Mixing of η, η' with $c\bar{c}, b\bar{b}$ states and their radiative decays*, *Nucl. Phys.* **B335** (1990) 101.
- [14] J. P. Ma, *Reexamining radiative decays of 1^{--} quarkonium into η' and η* , *Phys. Rev.* **D65** (2002) 097506, [[hep-ph/0202256](#)].
- [15] Y.-D. Yang, *Radiative decays $J/\psi \rightarrow \eta^{(\prime)}\gamma$ in perturbative QCD*, [hep-ph/0404018](#).
- [16] G. Li, T. Li, X.-Q. Li, W.-G. Ma, and S.-M. Zhao, *Revisiting the OZI-forbidden radiative decays of orthoquarkonia*, *Nucl. Phys.* **B727** (2005) 301, [[hep-ph/0505158](#)].
- [17] B. A. Li, *$\Upsilon(1s) \rightarrow \gamma(\eta', \eta)$ decays*, *Phys. Rev.* **D77** (2008) 097502, [[arXiv:0712.4246](#)].

- [18] J.-K. He and Y.-D. Yang, *Revisiting the radiative decays $J/\psi \rightarrow \gamma\eta^{(\prime)}$ in perturbative QCD*, *Nucl. Phys.* **B943** (2019) 114627, [[arXiv:1903.11430](#)].
- [19] T. Feldmann, P. Kroll, and B. Stech, *Mixing and decay constants of pseudoscalar mesons*, *Phys. Rev.* **D58** (1998) 114006, [[hep-ph/9802409](#)].
- [20] R. Barbieri, R. Gatto, and E. Remiddi, *Singular Binding Dependence in the Hadronic Widths of 1^{++} and 1^{+-} Heavy Quark anti-Quark Bound States*, *Phys. Lett.* **B61** (1976) 465.
- [21] R. Barbieri, M. Caffo, R. Gatto, and E. Remiddi, *Strong QCD Corrections to p Wave Quarkonium Decays*, *Phys. Lett.* **B95** (1980) 93.
- [22] R. Barbieri, M. Caffo, R. Gatto, and E. Remiddi, *QCD CORRECTIONS TO P WAVE QUARKONIUM DECAYS*, *Nucl. Phys.* **B192** (1981) 61.
- [23] W. Kwong, P. B. Mackenzie, R. Rosenfeld, and J. L. Rosner, *Quarkonium Annihilation Rates*, *Phys. Rev.* **D37** (1988) 3210.
- [24] G. T. Bodwin, E. Braaten, and G. P. Lepage, *Rigorous QCD predictions for decays of P wave quarkonia*, *Phys. Rev.* **D46** (1992) R1914, [[hep-lat/9205006](#)].
- [25] G. T. Bodwin, E. Braaten, and G. P. Lepage, *Rigorous QCD analysis of inclusive annihilation and production of heavy quarkonium*, *Phys. Rev.* **D51** (1995) 1125, [[hep-ph/9407339](#)]. [Erratum: *Phys. Rev.* **D55**, 5853 (1997)].
- [26] R. Zhu and J.-P. Dai, *Radiative $h_{c/b}$ decays to η or η'* , *Phys. Rev.* **D94** (2016) 094034, [[arXiv:1610.00288](#)].
- [27] C.-J. Fan and J.-K. He, *The radiative decays of h_c to the light mesons $\eta^{(\prime)}$: a perturbative QCD calculation*, *Phys. Rev.* **D100** (2019) 034005, [[arXiv:1906.07353](#)].
- [28] H.-W. Huang, C.-F. Qiao, and K.-T. Chao, *Electromagnetic annihilation rates of χ_{c0} and χ_{c2} with both relativistic and QCD radiative corrections*, *Phys. Rev.* **D54** (1996) 2123–2131, [[hep-ph/9601380](#)].

- [29] P. Kroll, *Exclusive charmonium decays*, *Nucl. Phys. Proc. Suppl.* **64** (1998) 456, [hep-ph/9709393].
- [30] S. M. H. Wong, *Color octet contribution to exclusive P wave charmonium decay into nucleon - anti-nucleon*, *Nucl. Phys. Proc. Suppl.* **74** (1999) 231, [hep-ph/9809447].
- [31] S. M. H. Wong, *Color octet contribution in exclusive P wave charmonium decay into proton - anti-proton*, *Nucl. Phys.* **A674** (2000) 185, [hep-ph/9903221].
- [32] S. M. H. Wong, *Color octet contribution in exclusive p wave charmonium decay into octet and decuplet baryons*, *Eur. Phys. J.* **C14** (2000) 643, [hep-ph/9903236].
- [33] S. M. H. Wong, *Color octet contribution in exclusive P wave charmonium decay*, *Nucl. Phys. Proc. Suppl.* **93** (2001) 220, [hep-ph/0009016]. [,220(2000)].
- [34] J. P. Ma and Q. Wang, *Corrections for two photon decays of χ_{c0} and χ_{c2} and color octet contributions*, *Phys. Lett.* **B537** (2002) 233, [hep-ph/0203082].
- [35] G.-L. Wang, *Annihilation rate of heavy 0^{++} P-wave quarkonium in relativistic Salpeter method*, *Phys. Lett.* **B653** (2007) 206, [arXiv:0708.3516].
- [36] G.-L. Wang, *Annihilation Rate of 2^{++} Charmonium and Bottomonium*, *Phys. Lett.* **B674** (2009) 172, [arXiv:0904.1604].
- [37] C.-W. Hwang and R.-S. Guo, *Two-photon and two-gluon decays of p-wave heavy quarkonium using a covariant light-front approach*, *Phys. Rev.* **D82** (2010) 034021, [arXiv:1005.2811].
- [38] A. N. Mitra and S. Bhatnagar, *Hadron - quark vertex function. Interconnection between 3D and 4D wave function*, *Int. J. Mod. Phys.* **A7** (1992) 121.
- [39] S. Bhatnagar, S.-Y. Li, and J. Mahecha, *power counting of various Dirac covariants in hadronic Bethe-Salpeter wave functions for decay constant calculations of pseudoscalar mesons*, *Int. J. Mod. Phys.* **E20** (2011) 1437, [arXiv:0912.3081].

- [40] S. Bhatnagar, J. Mahecha, and Y. Mengesha, *Relevance of various Dirac covariants in hadronic Bethe-Salpeter wave functions in electromagnetic decays of ground state vector mesons*, *Phys. Rev.* **D90** (2014) 014034, [[arXiv:1307.4044](#)].
- [41] E. Mengesha and S. Bhatnagar, *Cross section for double charmonium production in electron-positron annihilation at energy $\sqrt{s}=10.6$ GeV*, *Int. J. Mod. Phys.* **E20** (2011) 2521, [[arXiv:1105.4944](#)].
- [42] H. Negash and S. Bhatnagar, *Mass spectrum and leptonic decay constants of ground and radially excited states of η_c and η_b in a Bethe-Salpeter equation framework*, *Int. J. Mod. Phys.* **E24** (2015) 1550030.
- [43] H. Negash and S. Bhatnagar, *Spectroscopy of ground and excited states of pseudoscalar and vector charmonium and bottomonium*, *Int. J. Mod. Phys.* **E25** (2016) 1650059, [[arXiv:1508.06131](#)].
- [44] S. Bhatnagar and L. Alemu, *Approach to calculation of mass spectra and two-photon decays of $c\bar{c}$ mesons in the framework of Bethe-Salpeter equation*, *Phys. Rev.* **D97** (2018) 034021, [[arXiv:1610.03234](#)].
- [45] E. Gebrehana, S. Bhatnagar, and H. Negash, *Analytic approach to calculations of mass spectra and decay constants of heavy-light quarkonia in the framework of Bethe-Salpeter equation*, *Phys. Rev.* **D100** (2019) 054034, [[arXiv:1901.01888](#)].
- [46] C. H. Llewellyn-Smith, *A relativistic formulation for the quark model for mesons*, *Annals Phys.* **53** (1969) 521.
- [47] V. Sauli, *Bethe-Salpeter Study of Radially Excited Vector Quarkonia*, *Phys. Rev.* **D86** (2012) 096004, [[arXiv:1112.1865](#)].
- [48] V. Sauli and P. Bicudo, *Excited charmonium states from Bethe-Salpeter equation*, *PoS QCD-TNT-II* (2011) 043, [[arXiv:1112.5540](#)].
- [49] J. Resag, C. R. Munz, B. C. Metsch, and H. R. Petry, *Analysis of the instantaneous Bethe-Salpeter equation for $q\bar{q}$ bound states*, *Nucl. Phys.* **A578** (1994) 397, [[nucl-th/9307026](#)].

- [50] K.-T. Chao, H.-W. Huang, and Y.-Q. Liu, *Gluonic and leptonic decays of heavy quarkonia and the determination of $\alpha_s(m_c)$ and $\alpha_s(m_b)$* , *Phys. Rev.* **D53** (1996) 221, [[hep-ph/9503201](#)].
- [51] E. Eichten and F. Feinberg, *Spin Dependent Forces in QCD*, *Phys. Rev.* **D23** (1981) 2724.
- [52] W.-Y. Keung and I. J. Muzinich, *Beyond the Static Limit for Quarkonium Decays*, *Phys. Rev.* **D27** (1983) 1518.
- [53] R. Gupta, D. Daniel, and J. Grandy, *Bethe-Salpeter amplitudes and density correlations for mesons with Wilson fermions*, *Phys. Rev.* **D48** (1993) 3330, [[hep-lat/9304009](#)].
- [54] V. L. Chernyak and A. R. Zhitnitsky, *Asymptotic Behavior of Exclusive Processes in QCD*, *Phys. Rept.* **112** (1984) 173.
- [55] A. Ali and A. Ya. Parkhomenko, *The $\eta' g^* g^{(*)}$ vertex including the η' -meson mass*, *Eur. Phys. J.* **C30** (2003) 367, [[hep-ph/0307092](#)].
- [56] P. Ball and G. W. Jones, *$B \rightarrow \eta^{(\prime)}$ Form Factors in QCD*, *JHEP* **08** (2007) 025, [[arXiv:0706.3628](#)].
- [57] T. Muta and M.-Z. Yang, *$\eta' - g^* - g$ transition form factor with gluon content contribution tested*, *Phys. Rev.* **D61** (2000) 054007, [[hep-ph/9909484](#)].
- [58] M.-Z. Yang and Y.-D. Yang, *Revisiting charmless two-body B decays involving η' and η* , *Nucl. Phys.* **B609** (2001) 469, [[hep-ph/0012208](#)].
- [59] A. Ali and Ya. Parkhomenko, *The $\eta' g^* g^*$ vertex with arbitrary gluon virtualities in the perturbative QCD hard scattering approach*, *Phys. Rev.* **D65** (2002) 074020, [[hep-ph/0012212](#)].
- [60] S. S. Agaev, V. M. Braun, N. Offen, F. A. Porkert, and A. Schäfer, *Transition form factors $\gamma^* \gamma \rightarrow \eta$ and $\gamma^* \gamma \rightarrow \eta'$ in QCD*, *Phys. Rev.* **D90** (2014) 074019, [[arXiv:1409.4311](#)].
- [61] H. H. Patel, *Package-X: A Mathematica package for the analytic calculation of one-loop integrals*, *Comput. Phys. Commun.* **197** (2015) 276, [[arXiv:1503.01469](#)].

- [62] H. H. Patel, *Package-X 2.0: A Mathematica package for the analytic calculation of one-loop integrals*, *Comput. Phys. Commun.* **218** (2017) 66, [[arXiv:1612.00009](#)].
- [63] P. Kroll and K. Passek-Kumerički, *The two gluon components of the η and η' mesons to leading twist accuracy*, *Phys. Rev.* **D67** (2003) 054017, [[hep-ph/0210045](#)].
- [64] S. Alte, M. König, and M. Neubert, *Exclusive Radiative Z-Boson Decays to Mesons with Flavor-Singlet Components*, *JHEP* **02** (2016) 162, [[arXiv:1512.09135](#)].
- [65] **Particle Data Group** Collaboration, M. Tanabashi et al., *Review of Particle Physics*, *Phys. Rev.* **D98** (2018) 030001.
- [66] T. Feldmann, P. Kroll, and B. Stech, *Mixing and decay constants of pseudoscalar mesons: The Sequel*, *Phys. Lett.* **B449** (1999) 339, [[hep-ph/9812269](#)].
- [67] T. Feldmann, *Quark structure of pseudoscalar mesons*, *Int. J. Mod. Phys.* **A15** (2000) 159, [[hep-ph/9907491](#)].
- [68] R. Escribano and J.-M. Frère, *Study of the $\eta - \eta'$ system in the two mixing angle scheme*, *JHEP* **06** (2005) 029, [[hep-ph/0501072](#)].
- [69] T. Huang and X.-G. Wu, *Determination of the η and η' Mixing Angle from the Pseudoscalar Transition Form Factors*, *Eur. Phys. J.* **C50** (2007) 771, [[hep-ph/0612007](#)].
- [70] **UKQCD** Collaboration, E. B. Gregory, A. C. Irving, C. M. Richards, and C. McNeile, *A study of the η and η' mesons with improved staggered fermions*, *Phys. Rev.* **D86** (2012) 014504, [[arXiv:1112.4384](#)].
- [71] F.-G. Cao, *Determination of the η - η' mixing angle*, *Phys. Rev.* **D85** (2012) 057501, [[arXiv:1202.6075](#)].
- [72] R. Escribano, P. Masjuan, and P. Sanchez-Puertas, *η and η' transition form factors from rational approximants*, *Phys. Rev.* **D89** (2014) 034014, [[arXiv:1307.2061](#)].
- [73] **ETM** Collaboration, K. Ottnad and C. Urbach, *Flavor-singlet meson decay constants from $N_f = 2 + 1 + 1$ twisted mass lattice QCD*, *Phys. Rev.* **D97** (2018) 054508, [[arXiv:1710.07986](#)].

- [74] **BaBar** Collaboration, B. Aubert et al., *Measurement of the η and η' transition form-factors at $q^2 = 112 \text{ GeV}^2$* , *Phys. Rev.* **D74** (2006) 012002, [[hep-ex/0605018](#)].
- [75] **KLOE-2** Collaboration, D. Babusci et al., *Measurement of η meson production in $\gamma\gamma$ interactions and $\Gamma(\eta \rightarrow \gamma\gamma)$ with the KLOE detector*, *JHEP* **01** (2013) 119, [[arXiv:1211.1845](#)].
- [76] R. Escribano and J. M. Frere, *Phenomenological evidence for the energy dependence of the $\eta - \eta'$ mixing angle*, *Phys. Lett.* **B459** (1999) 288, [[hep-ph/9901405](#)].